

# Sym004: A Novel Synergistic Anti–Epidermal Growth Factor Receptor Antibody Mixture with Superior Anticancer Efficacy

Mikkel Wandahl Pedersen, Helle Jane Jacobsen, Klaus Koefoed, Adam Hey, Charles Pyke, John Sørensen Haurum, and Michael Kragh

## Abstract

Epidermal growth factor receptor (EGFR) is a validated therapeutic target in cancer and EGFR antagonists with greater effectiveness than existing clinical agents remain of interest. Here, we report a novel approach based on Sym004, a mixture of two anti-EGFR monoclonal antibodies directed against distinct nonoverlapping epitopes in EGFR extracellular domain III. Like anti-EGFR monoclonal antibodies in current clinical use, Sym004 inhibits cancer cell growth and survival by blocking ligand-binding receptor activation and phosphorylation and downstream receptor signaling. However, unlike the other antibodies, Sym004 induces rapid and efficient removal of the receptor from the cancer cell surface by triggering EGFR internalization and degradation. Compared with reference anti-EGFR monoclonal antibodies, Sym004 exhibited more pronounced growth inhibition *in vitro* and superior efficacy *in vivo*. Together, these findings illustrate a strategy to target EGFR more effectively than existing clinical antibodies. *Cancer Res*; 70(2); 588–97. ©2010 AACR.

## Introduction

The epidermal growth factor receptor (EGFR; ErbB1) signaling system is frequently unbalanced in human malignancies due to increased ligand production, receptor overexpression, receptor mutations, and/or cross-talk with other receptor systems (1–3). Changes in EGFR status have been linked to the development and maintenance of a malignant phenotype and correlated to poor clinical prognosis (4). For this reason, the EGFR is an attractive target for anticancer therapy (5).

Currently, two monoclonal antibodies (mAbs) targeting the EGFR, cetuximab (Erbix) and panitumumab (Vectibix), are approved for the treatment of metastatic colorectal cancer and additional mAbs are in clinical development for various indications (6).

Cetuximab and panitumumab have been shown to inhibit ligand binding, receptor heterodimerization, and downstream signaling by binding to extracellular domain III of the EGFR (7). mAb-mediated engagement of immunologic effector cells by FcγR binding resulting in antibody-dependent cellular cytotoxicity toward the tumor is another proposed mechanism of cetuximab (8). Anti-EGFR mAbs have also

been implicated in acceleration of EGFR internalization. This mechanism is particularly attractive as it mimics ligand-induced endocytosis and degradation of active EGFRs, an important native state physiologic process responsible for attenuation of growth-promoting signals (9). Recently, it has been shown that certain combinations of antibodies can be considerably more potent at inducing downregulation of receptor tyrosine kinases and that such antibody mixtures may be superior at controlling tumor growth (10, 11).

Here, we present a novel antibody mixture containing two antibodies targeting the EGFR and with superior anticancer efficacy compared with existing mAbs. Using the mSymplex technology, we identified a comprehensive repertoire of EGFR-specific antibodies from which a diverse subset was characterized in detail. Using an efficacy-based approach, >400 different antibody combinations were tested in a standard viability assay *in vitro*. Three lead candidate mixtures with high efficacy *in vitro* were selected and tested for their ability to inhibit tumor growth *in vivo*.<sup>1</sup> A combination of two antibodies, 992 and 1024, was identified as the most potent and having the highest efficacy of all combinations both *in vitro* and *in vivo*. This mixture is referred to as Sym004. The two antibodies in Sym004 are directed against distinct epitopes on the extracellular domain of EGFR. Here, we present data from the functional characterization of Sym004.

**Authors' Affiliation:** Symphogen A/S, Lyngby, Denmark

**Note:** Supplementary data for this article are available at Cancer Research Online (<http://cancerres.aacrjournals.org/>).

**Corresponding Author:** Mikkel Wandahl Pedersen, Department of Antibody Pharmacology, Symphogen A/S, Elektrovej Building 375, DK-2800 Lyngby, Denmark. Phone: 45-45266349; Fax: 45-45265060; E-mail: mwp@symphogen.com.

doi: 10.1158/0008-5472.CAN-09-1417

©2010 American Association for Cancer Research.

<sup>1</sup> K. Koefoed et al. Identification of a highly efficacious dual antibody mixture targeting the epidermal growth factor receptor, submitted for publication.

## Materials and Methods

**Materials.** Anti-EGFR mAbs cetuximab (Erbix, Merck) and panitumumab (Vectibix, Amgen) and negative control anti-respiratory syncytial virus mAb Synagis (Abbott) were used. The mSymplex identification, cloning, and characterization of the 992, 1024, and 1030 antibodies are described by Koefoed and colleagues.<sup>1</sup> The mSymplex technology is a murine variant of the Symplex technology used for human B cells (12). The mSymplex method is a PCR-based method for cloning of antibodies from single-sorted murine plasma cells. Due to the single PCR step, the natural heavy and light chain pairing is maintained for the antibodies. The antibodies 992 and 1024 were stored individually at  $-80^{\circ}\text{C}$  or at  $4^{\circ}\text{C}$  for shorter periods. Before performing experiments, the two antibodies were mixed in a ratio of 1:1 (w/w) and immediately thereafter added to experimental wells or injected into mice. Antibodies against phosphorylated EGFR (pEGFR; Tyr<sup>845</sup>), pEGFR (Tyr<sup>1045</sup>), pEGFR (Tyr<sup>1068</sup>), phosphorylated extracellular signal-regulated kinase (pERK) 1/2 (Thr<sup>202</sup>/Thr<sup>204</sup>), ERK1/2, AKT, phosphorylated AKT (pAKT; Ser<sup>473</sup>), PDK1, phosphorylated PDK1 (Ser<sup>241</sup>), S6R, phosphorylated S6R (pS6R), p21CIP, and  $\beta$ -actin were purchased from Cell Signaling Technology. Sheep anti-human EGFR was from Fitzgerald, horseradish peroxidase (HRP)-conjugated secondary antibodies were from DakoCytomation, and 800CW-conjugated secondary antibodies were from LI-COR Biosciences.

**Cell lines.** The following cancer cell lines were obtained from the American Type Culture Collection: A431, A431NS, A549, AU565, BT20, BT474, CALU3, DU145, H1975, H292, HCC827, HT29, MDA-MB-468, Mia-PACA2, PC3, SKBR3, and SKOV3. The A431NS cell line was derived from the parental cell line A431 in 1997 by repeated subculturing to select cells that detach from the substrate easily (13). The A431 and A431NS cell lines have similar levels of EGFR, pEGFR, and HER2, but A431NS has a higher rate of proliferation *in vitro* and is more aggressive *in vivo*.

The cell line HN5 was from the Department of Radiation Biology, Copenhagen University Hospital (Copenhagen, Denmark). The colon cancer cell line GEO has been described previously (14) and was a generous gift from Professor Douglas Boyd (M.D. Anderson Cancer Center, Houston, TX). All cells were maintained in appropriate medium supplemented with 10% fetal bovine serum (FBS), 50 units/mL penicillin, and 50  $\mu\text{g}/\text{mL}$  streptomycin.

**Surface plasmon resonance analysis.** A ProteOn XPR36 (Bio-Rad) biosensor was used for surface plasmon resonance (SPR) analysis. Anti-human IgG (Fc) antibody (GE Healthcare) was conjugated to a GLC chip (Bio-Rad) using the manufacturer's recommendations and a flow rate of 25  $\mu\text{L}/\text{min}$ . Soluble EGFR (sEGFR) fused to human IgG Fc (R&D Systems) was captured on the anti-Fc surface followed by injections of saturating concentrations of antibody pairs (40  $\mu\text{g}/\text{mL}/267$  nmol/L). The surface was regenerated by a 30-s injection of 3 mmol/L  $\text{MgCl}_2$ .

**Viability assay.** Three-fold serial dilutions of antibodies were prepared in triplicate in 96-well plates, and cancer cells were added in medium containing 0.5% FBS. After 96 h, the

number of viable cells was measured using the WST-1 Cell Proliferation Reagent (Roche Diagnostics) according to the manufacturer's instructions.

**Xenograft studies.** Cells (A431NS:  $10^6$ ; HN5:  $\sim 2 \times 2 \times 2$  mm tumor fragment; H1975:  $2 \times 10^6$ ; or HCC827:  $5 \times 10^6$ ) suspended in 0.1 mL PBS were inoculated s.c. into the right flank of 6- to 8-wk-old BALB/c *nu/nu* mice. Mice were monitored daily, and tumors were measured two to three times weekly using calipers. Tumor volumes were calculated using the following formula:  $1/2 \times L \times W^2$  ( $L$  = length;  $W$  = width). Antibodies were administered at 25 or 50 mg/kg twice weekly by i.p. injection. The results are expressed as mean  $\pm$  SE, and statistical significance was analyzed using ANOVA followed by a Student's *t* test. The tumor volume of animals excluded before termination of the study was carried through. All *in vivo* studies were performed in accordance with the Danish law on animal experimentation and approved by the Animal Ethical Committee, Denmark.

**Immunofluorescence confocal microscopy.** Antibodies were labeled with either Alexa Fluor 488 or Alexa Fluor 647 using antibody labeling kits (Invitrogen). For the internalization assays, cells were treated with labeled antibodies, fixed with 4% formaldehyde, and stained with 1  $\mu\text{mol}/\text{L}$  Hoechst (Invitrogen) and 2  $\mu\text{g}/\text{mL}$  CellMask Blue (Invitrogen). For the EGFR degradation assay, cells were treated with unlabeled antibodies, fixed in 4% formaldehyde, and then stained with Alexa Fluor 647-labeled mAb 1030 and a solution of 1  $\mu\text{mol}/\text{L}$  Hoechst and 2  $\mu\text{g}/\text{mL}$  CellMask Blue. Cells were examined using the Opera LX high-content confocal imaging system (Perkin-Elmer) at 400 $\times$  or 600 $\times$  or using an Olympus BX microscope. Image analyses were performed using Acella software (Perkin-Elmer). At least 100 cells were used for quantifications.

**Generation of Fab fragments.** Fab fragments of the antibodies 992 and 1024 were generated by papain digestion as described previously (15).

**Immunoblot analyses.** Protein levels were determined by preparing whole-cell lysates from cell lines and xenografts and analyzed by immunoblot as described previously (16).

Band intensities were quantified using the public domain Java image-processing program ImageJ.<sup>2</sup>

For analysis of EGFR signaling, cancer cells were serum starved overnight and pretreated with 10  $\mu\text{g}/\text{mL}$  of control mAb, Sym004, or cetuximab for 8 h and then left unstimulated or stimulated with 1 nmol/L EGF (R&D Systems) for 7.5 min. Immunoblot analyses were performed with  $\beta$ -actin as loading control. Bands were visualized by addition of 800CW fluorescently labeled secondary antibodies and imaged using the Odyssey System (LI-COR Biosciences).

**Immunohistochemistry.** Tumor tissue samples were collected from A431NS xenografted tumors treated twice weekly with 50 mg/kg of control mAb, Sym004, or cetuximab for 3 wk. Tumor samples were fixed in 4% formaldehyde and paraffin embedded. The EGFR pharmDx kit using antibody 18C9

<sup>2</sup> <http://rsb.info.nih.gov/ij>

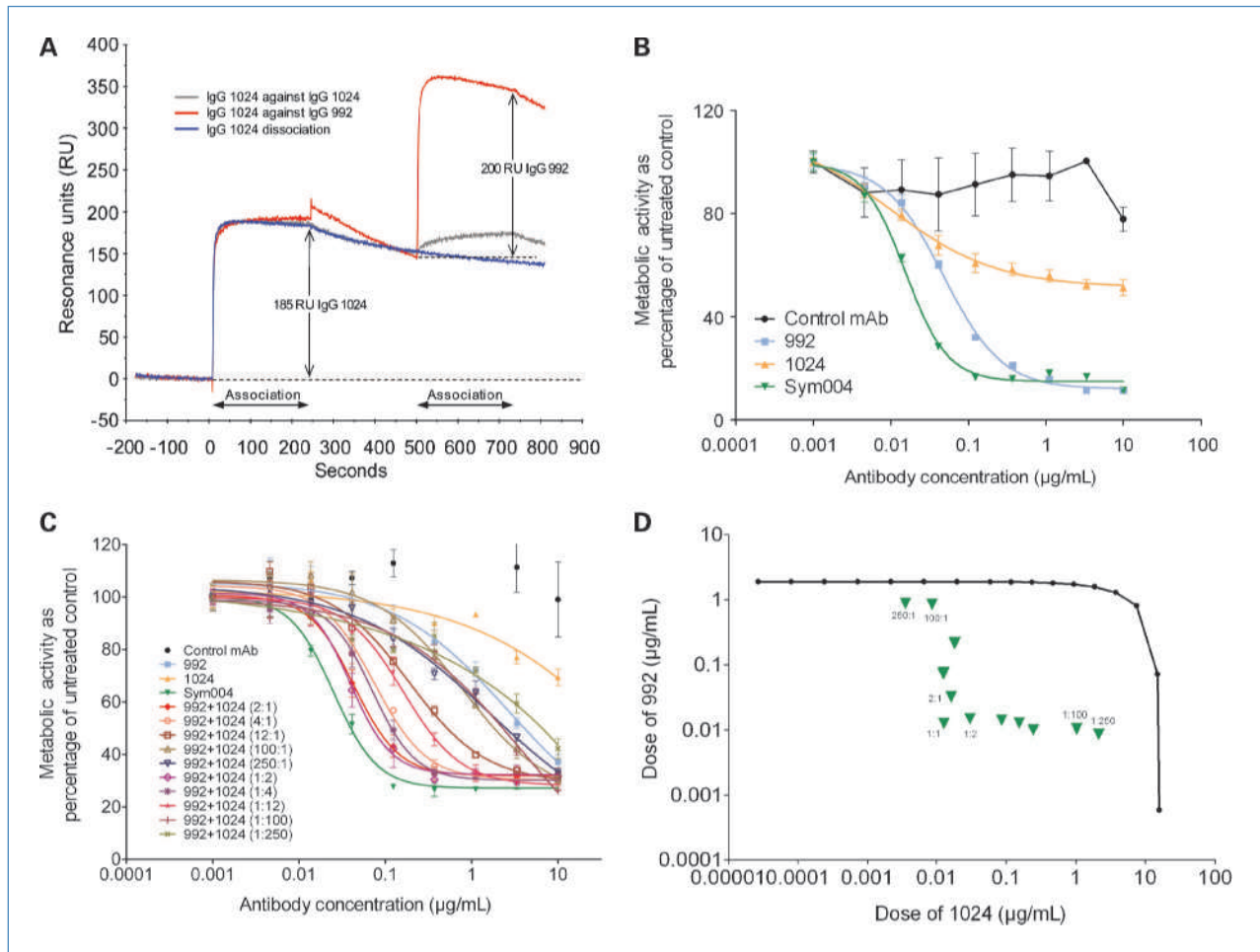


**Figure 1.** Properties of Sym004. **A**, overlay plots showing simultaneous binding of Sym004 to captured sEGFR determined by SPR analysis. Bound 1024 was allowed to dissociate (blue line), competed against itself (grey line), or competed against 992 (red line). **B**, metabolic activity of HCC827 cells treated with the indicated antibodies for 96 h. **C**, metabolic activity of A431NS cells treated with 992, 1024, or mixtures of the two antibodies in the indicated ratios for 96 h. **D**, analysis of synergy using isobologram. Black line, theoretical additive isobole for 50% inhibition of A431NS cell growth. The additive isobole represents all dose pairs of 992 and 1024 that, based on the above potencies, should give 50% growth inhibition. Green triangles, actual experimentally determined dose pairs of Sym004 that give a 50% effect level.

against EGFR and secondary HRP-conjugated goat anti-mouse IgG (DakoCytomation) was used according to the manufacturer's instructions to detect EGFR levels. Antibody binding was revealed by addition of 3,3'-diaminobenzidine substrate. Tissues were counterstained with Mayer's H&E stain (Bie and Berntsen). Tissues were examined using an Olympus BX51 microscope. Images were taken at 40× and 200×.

## Results

**Sym004 binds nonoverlapping epitopes in the EGFR extracellular domain.** Sym004 is a 1:1 mixture of the two chimeric IgG1 antibodies 992 and 1024, which have been shown to bind two distinct nonoverlapping epitopes on the extracellular domain III of EGFR with high affinities.<sup>1</sup> To confirm simultaneous binding of the two antibodies to EGFR, a surface

plasmon resonance analysis was performed measuring binding to the extracellular domain of EGFR. Figure 1A shows that the two antibodies can bind simultaneously to the extracellular domain of EGFR.

**Sym004 synergistically inhibits cancer cell growth in vitro.** The potency and efficacy of Sym004 in inhibiting cancer cell growth were investigated in a range of cancer cell lines of different tissue origin and with varying EGFR levels (see Supplementary Table S1 for IC<sub>50</sub> values). Eleven of the 19 cell lines tested were inhibited by Sym004, whereas only 7 cell lines were inhibited by the individual 992 and 1024 mAbs. An example of antibody-induced growth inhibition is shown for the HCC827 cell line in Fig. 1B. The results show that Sym004 is more potent at inhibiting the growth of this cell line compared with 992 and 1024.

The optimal ratio between 992 and 1024 in the mixture was tested in growth inhibition assays with A431NS and



HCC827 cells, respectively (Fig. 1C; Supplementary Fig. S1). In both cell lines, the 1:1 (w/w) mixture was the most potent and the  $IC_{50}$  increased when the ratio was altered toward 1:250 or 250:1. However, the effect of the antibody combina-

tion on cell proliferation proved very robust over a wide range of ratios, as the initial decreases in potencies when moving away from the optimal 1:1 mixture were relatively small.

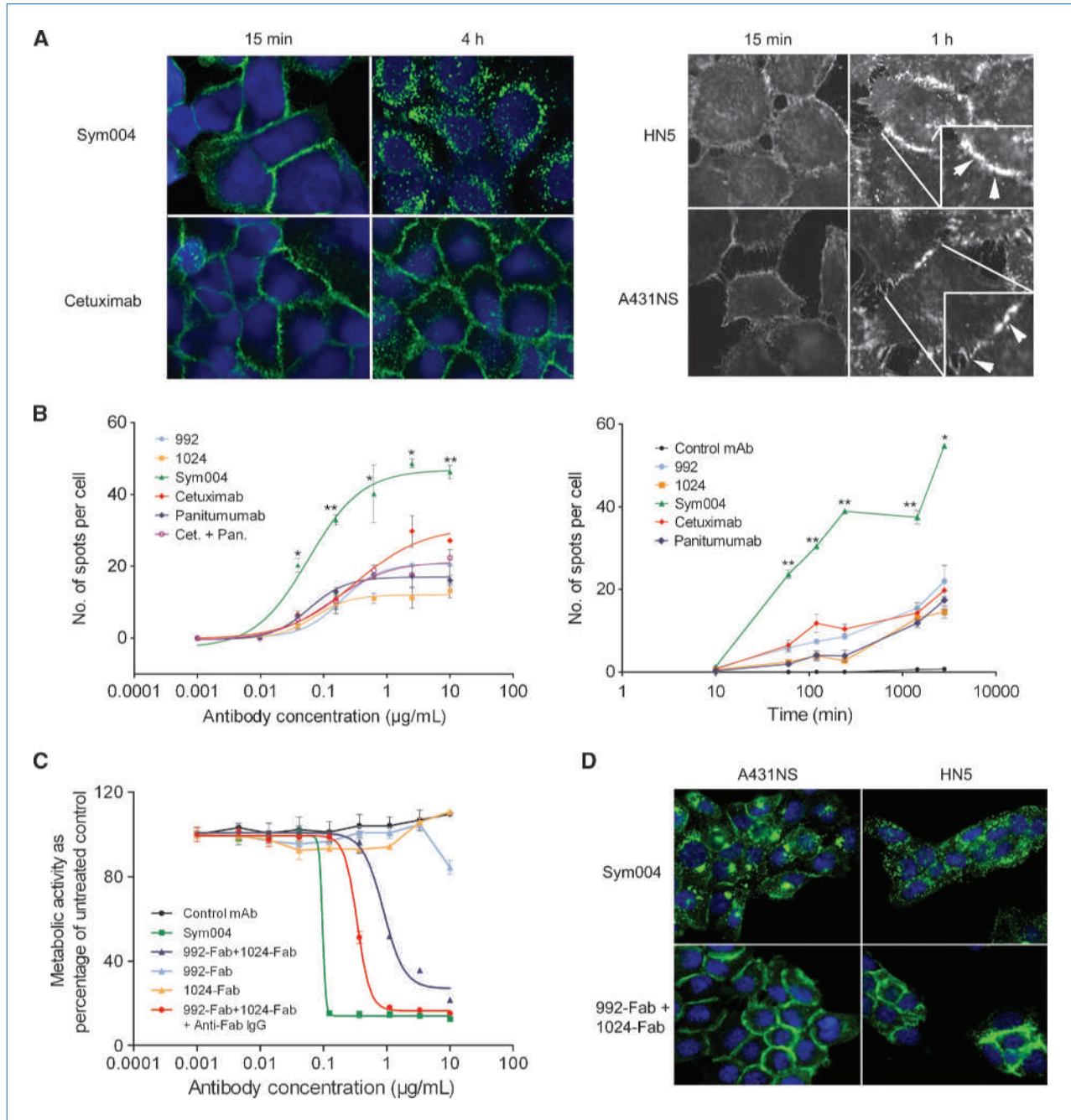


**Figure 2.** Sym004-induced internalization. *A*, confocal images (400 $\times$ ) of the location of Alexa Fluor 488-labeled Sym004 and cetuximab in HN5 cells after 15 min and 4 h of incubation (*left*) and confocal images of HN5 and A431NS cells treated with Sym004 for 15 min and 1 h taken at 600 $\times$  resolution (*right*). *White arrows*, Sym004-induced clustering of EGFR-antibody complexes at the cell surface of the cancer cells after 1 h of incubation. *B*, number of spots per cell after 4 h of treatment of HN5 cells with different concentrations of the indicated antibodies (*left*) or at different time points after treatment of HN5 cells with 10  $\mu\text{g/mL}$  of the indicated antibodies (*right*). *Points*, mean; *bars*, SE. \*,  $P < 0.05$ ; \*\*,  $P < 0.01$ , Student's *t* test, Sym004 versus cetuximab. *C*, metabolic activity of HN5 cells after 96 h of incubation with different concentrations of the indicated antibodies or Fab fragments. *D*, images of A431NS and HN5 cells treated with a mixture of either Alexa Fluor 488-labeled 992 and 1024 or Alexa Fluor 488-labeled Fab fragments of 992 and 1024 for 4 h. Images recorded at 400 $\times$  resolution.

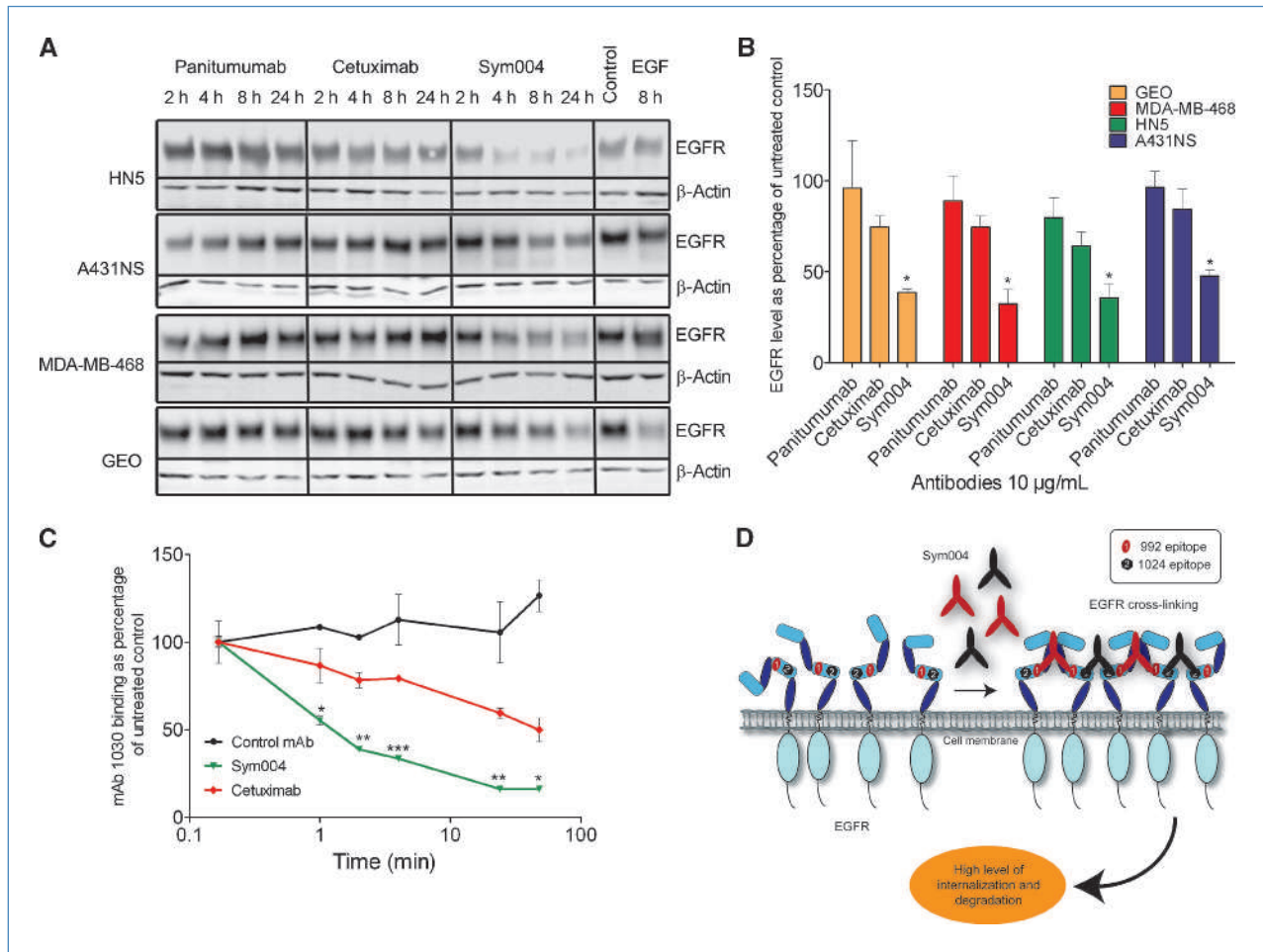


**Figure 3.** Sym004-induced EGFR degradation *in vitro*. **A**, immunoblot analyses of EGFR levels in HN5, A431NS, MDA-MB-468, and GEO cell lines after treatment with 10 µg/mL of the indicated antibodies. **B**, quantification of EGFR levels in cell lines after 24 h of antibody treatment relative to untreated control cells measured in arbitrary units from Western blots as in **A**. Columns, mean; bars, SD. \*,  $P < 0.05$ , Student's *t* test, Sym004 versus cetuximab. **C**, quantification of the level of mAb 1030 binding to HN5 cells from images taken at 400× after different treatment periods with either Sym004 or cetuximab. Points, mean; bars, SE. \*,  $P < 0.05$ ; \*\*,  $P < 0.01$ ; \*\*\*,  $P < 0.001$ , Student's *t* test, Sym004 versus cetuximab. **D**, proposed model for the Sym004 mechanism of action.

To investigate whether 992 and 1024 work in true synergy, the theoretically determined, so-called additive isobole at the 50% level of inhibition of A431NS cell growth ( $IC_{50}$ ) was calculated from the individual antibody titration curves (Fig. 1C), as described by Tallarida (17). Plotting the experimentally determined  $IC_{50}$  values for the A431NS cell growth inhibition for all dose pairs of 992 and 1024 in the isobologram (Fig. 1D) showed that they were significantly below the theoretically determined additive isobole, showing that the two antibodies act highly synergistically (17). It is also evident that the 1:1 ratio is the mixture displaying the strongest level of synergy, as it lies furthest away from the additive isobole (Fig. 1D).

**Sym004 induces efficient internalization of EGFR on cancer cells.** Cancer cell lines were treated with different concentrations of Alexa Fluor 488–labeled antibodies for varying periods of time (Fig. 2A). After 15 minutes of incuba-

tion, both Sym004 and cetuximab were located at the cell surface. Following a 4-hour incubation period, most of the reference mAb cetuximab was still located on the cell surface and cells contained only very few visible intracellular antibody-containing vesicles. In contrast, most of the antibody in Sym004-treated cells was located in intracellular vesicles. The Sym004-induced EGFR internalization was preceded by a clustering of receptor-antibody complexes at the cell surface, as shown in Fig. 2A (right).

Internalization was quantified by counting the number of visible vesicles in each cell section (Fig. 2B). Sym004-treated cells had a significantly higher number of vesicles (two to three times) in all concentrations tested, and they appeared much faster than in cells treated with mAbs. Maximal potency and efficacy of Sym004 were found to be dependent on the bivalency of the two antibodies because a mixture of 992 and 1024 Fab fragments was unable to inhibit the proliferation of

HN5 cells (Fig. 2C). Cross-linking of the Fab fragments with an anti-Fab IgG increased potency and maximized efficacy. In line with these observations, the Fab fragment mixture failed to induce EGFR internalization (Fig. 2D), whereas cross-linking of the Fab fragments partially restored the ability to internalize EGFR (data not shown).

**Sym004-induced internalization of EGFR is followed by receptor degradation.** The fate of internalized receptors was investigated by immunoblot analyses of EGFR levels in cancer cell lines treated with antibodies for 2, 4, 8, or 24 hours. The level of EGFR decreased drastically in all four Sym004-treated cell lines, whereas only a small decrease in EGFR levels was seen in cells treated with reference antibodies (Fig. 3A). Quantification of band intensities showed that Sym004 removed 50% to 70% of EGFRs within 24 hours in the four cell lines tested (Fig. 3B). A similar experiment was performed with the most internalization-resistant cell

line A431NS in the presence of the protein synthesis inhibitor cycloheximide. Under these conditions, Sym004 completely removed the EGFR from A431NS cells within 24 hours (see Supplementary Fig. S2). Thus, the apparent lower removal of EGFR in this cell line is due to high ongoing rate of EGFR protein synthesis. EGFR removal by Sym004 was verified using an Alexa Fluor 647-labeled mAb 1030, which is able to bind to the EGFR simultaneously with Sym004 or cetuximab. After 24 hours, Sym004 completely eliminated binding of mAb 1030 on HN5 cells, whereas mAb 1030 was still able to bind to cetuximab-treated cells (Fig. 3C). The difference between the two treatments was statistically significant after 1 hour.

**Sym004 is a potent inhibitor of tumor growth in a range of xenograft models.** To investigate whether the superior removal of EGFR from cancer cells by Sym004 *in vitro* could be translated into a superior antitumor response

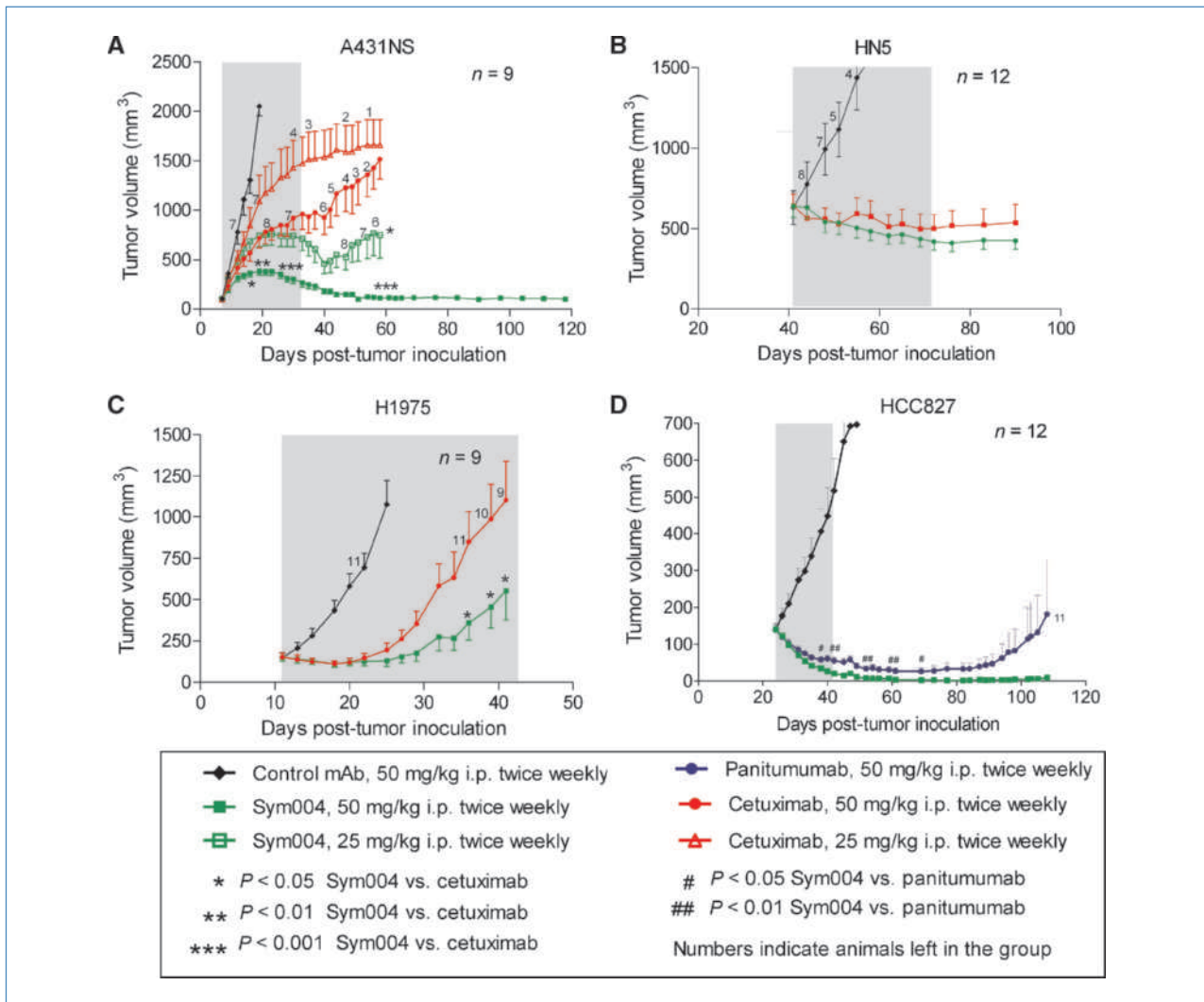


**Figure 4.** *In vivo* growth-inhibitory effect of Sym004 in xenografts. Growth-inhibitory effects of Sym004 in A431NS xenografts (A), HN5 xenografts (B), H1975 xenografts (C), and HCC827 xenografts (D). The number of mice in each group is shown at the top right corner of each figure, and the numbers next to the curves indicate the number of animals left in the treatment group.



*in vivo*, the efficacy of Sym004 was tested in several xenograft models. For comparison, one or both of the approved mAbs cetuximab and panitumumab were included in the studies (Fig. 4).

Initially, the effect of Sym004 on the growth of the very aggressive A431NS tumor xenografts was evaluated. Both Sym004 and cetuximab showed a clear dose response. However, cetuximab at both 25 and 50 mg/kg was only able to partially suppress the growth of A431NS tumors (Fig. 4A).

Treatment with 25 mg/kg Sym004 provided stronger tumor suppression compared with cetuximab, and treatment with 50 mg/kg Sym004 not only suppressed tumor growth but also induced complete tumor regression in all of the mice treated. No recurring tumors were detected at day 120 in any of the Sym004-treated mice, showing a long-lasting effect of the antibody treatment.

Sym004 and cetuximab were also compared in large tumor xenografts established from the head and neck cancer cell line HN5 (Fig. 4B). Here, Sym004 was able to control tumor growth with a slight decrease in average tumor volume, but the observed difference between Sym004 and cetuximab treatments was not statistically significant. To extend the observations to tumors of non-squamous origin, tumor xenografts established from the non-small cell lung cancer cell lines H1975 and HCC827 with average tumor volumes of 150 mm<sup>3</sup> were treated

with Sym004 and either cetuximab or panitumumab (Fig. 4C and D, respectively). In the H1975 xenograft model, Sym004 significantly delayed tumor growth compared with cetuximab. Sym004 at 50 mg/kg also caused rapid and complete regression of all tumors in the HCC827 xenograft model, with no evidence of tumor recurrence at day 110 after inoculation. Panitumumab was significantly less potent at controlling tumor growth, and tumor recurrence was detected in this treatment group 40 days after discontinuation of treatment.

**Sym004 causes complete removal of EGFR *in vivo*.** The ability of Sym004 to remove EGFR *in vivo* was investigated in A431NS tumors. The EGFR levels in individual tumors were evaluated by immunoblot analysis. Sym004-treated tumors were completely devoid of EGFR, whereas cetuximab-treated tumors contained significant levels of EGFR, although lower than control-treated tumors (Fig. 5A and B). These findings were verified in tissue sections of the tumors by immunohistochemical analysis of EGFR (Fig. 5C). Control mAb-treated tumors had large areas with viable A431NS cells with high levels of EGFR (dark brown areas). In cetuximab-treated tumors, keratin pearls were clearly visible (Fig. 5C, *black arrows*), but dispersed between these were large areas of viable tumor cells with high levels of EGFR expression. In contrast, Sym004-treated tumors contained no areas positive for EGFR and most of the tumor volume consisted of keratin (Fig. 5C).

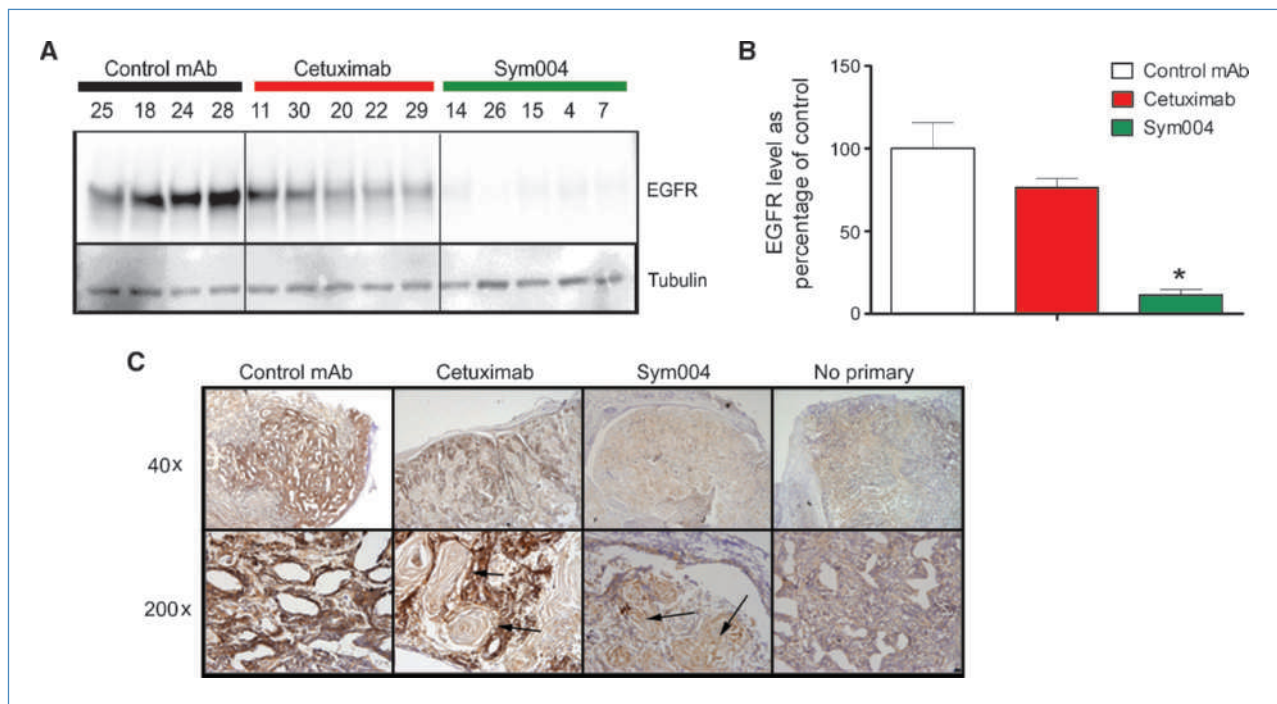


**Figure 5.** Sym004-induced EGFR degradation *in vivo*. **A**, immunoblot analyses of EGFR levels in five individual A431NS tumors after 3 wk of twice weekly injections with 50 mg/kg of a control mAb, cetuximab, or Sym004. **B**, quantification of EGFR levels in A431NS tumors relative to control-treated tumors measured in arbitrary units from Western blots as in **A**. Columns, mean; bars, SE. \*,  $P < 0.05$ , Student's *t* test, Sym004 versus cetuximab. **C**, immunohistochemical analysis of EGFR levels in the same A431NS tumors as in **A**. Dark brown color is indicative of high EGFR levels. Representative images taken at 40 $\times$  and 200 $\times$  resolution are shown.

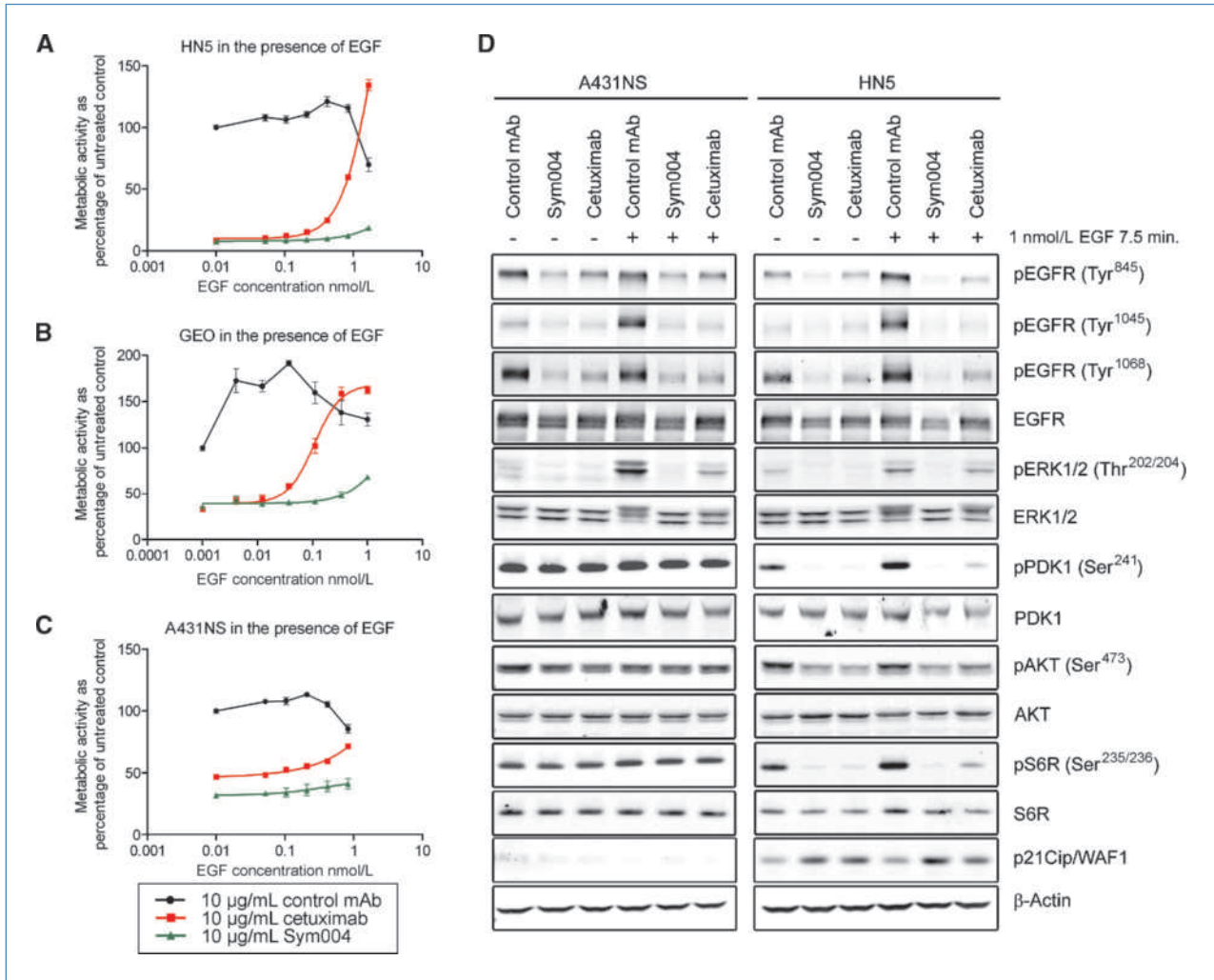


**Figure 6.** Sym004 is less sensitive to acquired resistance due to increased ligand levels. *A*, metabolic activity of HN5 head and neck cancer cells treated with 0 to 2 nmol/L of EGF and 10 µg/mL of control antibody, Sym004, or cetuximab after 96 h of treatment. *B*, metabolic activity of GEO colon cancer cells treated with 0 to 1 nmol/L of EGF and 10 µg/mL of control antibody, Sym004, or cetuximab after 96 h of treatment. *C*, metabolic activity of A431NS cells treated with 0 to 1 nmol/L of EGF and 10 µg/mL of control antibody, Sym004, or cetuximab after 96 h of treatment. *D*, immunoblot analyses of the effect of EGF stimulation on the phosphorylation of major signaling pathways downstream of EGFR—pEGFR, pERK, pAKT, and pS6R—following 8 h of treatment with 10 µg/mL of antibody. pPDK1, phosphorylated PDK1.

**Sym004 treatment is less sensitive to ligand-dependent resistance.** Acquired resistance to anti-EGFR antibody therapy caused by increased ligand production was modeled in a viability assay by addition of different concentrations of EGF to HN5, GEO, and A431NS cancer cells simultaneously with 10 µg/mL of antibody (Fig. 6A–C). Increasing amounts of EGF increased cell proliferation and made the cells completely or partially resistant to cetuximab treatment. Sym004 potentially inhibited proliferation of these cell lines in the presence of EGF, showing that removal of EGFR from the cancer cells is a more efficient way of blocking ligand-induced proliferation.

**Sym004-induced downregulation of EGFR inhibits ligand-induced phosphorylation of downstream signaling molecules.** To further investigate the mechanisms underly-

ing the superior inhibitory potential of Sym004 in the presence of ligand, phosphorylation of EGFR and downstream signaling molecules was investigated in the cell lines A431NS and HN5 (Fig. 6D). In the presence and absence of ligand, Sym004 treatment led to a more potent blockade of EGFR phosphorylation at the sites Tyr<sup>845</sup>, Tyr<sup>1045</sup>, and Tyr<sup>1068</sup> compared with cetuximab. Similar results were found for phosphorylation of ERK in the presence of ligand. Sym004 was also more potent than cetuximab in inhibiting phosphorylation of AKT, PDK1, and S6R in the HN5 cell line, whereas these molecules were constitutively phosphorylated and unresponsive to anti-EGFR antibodies in the A431NS cell line. Sym004 treatment also led to superior induction of the cell cycle inhibitor p21CIP/WAF1 in the HN5 cell line.



## Discussion

Development of more efficacious cancer treatment is important to effectively treat and hopefully cure more patients. With the aim of identifying anti-EGFR antibody mixtures with superior efficacy over mAbs, we screened a large panel of mAb mixtures for high antiproliferative activity *in vitro* and *in vivo*.<sup>1</sup> Sym004 was identified as the most potent and efficacious combination and consists of an equal amount of the two mAbs 992 and 1024.

In the current work, we show that 992 and 1024 work highly synergistically when combined. The synergy is due to very efficient induction of EGFR internalization and subsequent degradation, as shown in a range of cancer cell lines of different tissue origin. Internalization was preceded by formation of antibody-EGFR complexes at the cell surface, presumably caused by cross-linking of receptors by the antibodies, as previously suggested by Friedman and colleagues (10), as a general mechanism of action for antibodies with nonoverlapping epitopes binding to receptor tyrosine kinases. Further, evidence that cross-linking of EGFR is involved in Sym004-induced internalization is provided by the observation that a mixture of 992- and 1024-derived Fab fragments failed to induce EGFR internalization.

The internalization of EGFR by Sym004 is a prerequisite for efficient tumor cell growth inhibition, as shown in a viability assay using Fab fragments of 992 and 1024. The Fab fragment mixture was a much weaker inhibitor of cancer cell growth than full-length Sym004. Addition of an anti-Fab bridging antibody partially restored both the potency and the efficacy of the Fab mixture, and this correlated with increased internalization. Thus, receptor cross-linking by Sym004 followed by target internalization seems to be a prerequisite for the observed synergy and maximum potency and efficacy of the mixture (Fig. 3D).

Normally, ligand binding to the EGFR induces rapid internalization, which is followed by recycling of the receptor to the cell surface or degradation in lysosomes depending on the signal intensity and the cellular context (18–21). Sym004-induced internalization of EGFR is slower than ligand-induced internalization and is independent of EGFR tyrosine kinase activity, as shown using the selective tyrosine kinase inhibitor AG1478 (Supplementary Fig. S3). In contrast to ligand-induced internalization, Sym004-induced internalization of EGFR is always followed by degradation of the receptor and the bound antibody.

The susceptibility of the EGFR to undergo internalization and degradation following antibody treatment differed among the cancer cell lines tested. Although the cell lines HN5 and A431NS express approximately equal levels of EGFR, the receptor was internalized and degraded more rapidly in HN5 cells compared with A431NS cells.

Despite the slower speed of EGFR downregulation by Sym004 on A431NS cells, the removal of EGFR is crucial for obtaining maximum efficacy in this cell line. The lack of sufficient internalization and degradation of EGFR on A431NS cells by mAbs such as cetuximab may explain its partial resistance to anti-EGFR mAb therapy both *in vitro* and *in vivo*. The

fact that cross-linking of cetuximab by anti-human IgG leads to increased EGFR internalization and an efficacy comparable with that of Sym004 supports this hypothesis (Supplementary Fig. S4). The reason for the decreased rate of EGFR removal by Sym004 from A431NS cells may be either a failure in the downregulation machinery or compensatory augmented synthesis of EGFR. The observation that inhibition of new protein synthesis by cycloheximide addition leads to complete removal of EGFR in A431NS cells by Sym004 favors the latter explanation (Supplementary Fig. S2). Examination of the antitumor activity of Sym004 in multiple mouse tumor xenograft models (Fig. 4) confirmed the unique antitumor properties of Sym004. Tumor eradication of A431NS and HCC827 xenografts was achieved in all of the mice treated. Furthermore, no signs of tumor regrowth were observed in the study periods. In the A431NS tumors, even the low dose of Sym004 was significantly more potent at inhibiting tumor growth than the high dose of cetuximab. In the two lung cancer xenograft models H1975 and HCC827, Sym004 was significantly more potent at inhibiting tumor growth than cetuximab and panitumumab, respectively. The lack of a statistically significant difference between Sym004 and cetuximab in the HN5 model was unexpected but not surprising, as *in vitro* data have shown that Sym004 and cetuximab are equally effective at inhibiting the growth of HN5 in the absence of the ligand (Fig. 6A). The lack of superiority of Sym004 at inhibiting the growth of HN5 cells indicates that complete EGFR internalization and degradation is superfluous for maximum inhibition of this cell line in the absence of the ligand. The availability of ligands in the xenograft model thus seems limited.

The currently used therapeutic mAbs targeting EGFR function primarily by blocking access of ligands to the ligand-binding area of the receptor and, to a lesser extent, by inducing receptor internalization and degradation (9). Efficient removal of the receptor from the cancer cell will eliminate all interactions of EGFR with other proteins, including those that are independent of the receptor tyrosine kinase (22). Elimination of all EGFR-dependent interactions may in turn result in a superior antitumor response and a reduced ability of tumor cells to acquire resistance to treatment. Of particular relevance in this context is the reinstatement of ligand-induced receptor signaling that can be observed in the presence of mAbs by a compensatory upregulation of EGFR ligands. Ligands compete with the mAbs for binding to EGFR at the cancer cell surface, resulting in treatment desensitization or resistance. Furthermore, the EGFR dimerization induced by the mAbs may lower the threshold for ligand activation. The results presented here indicate that ligand is able to cause resistance to mAb therapy and that Sym004 can overcome this mechanism of resistance from the competing ligand by effectively removing the receptor from the cell surface. In line with these data, it was shown that Sym004 was superior to cetuximab at inhibiting EGFR phosphorylation and downstream signaling to ERK1/2, PDK1, AKT, and S6R in human cancer cell lines.

Interaction of EGFR with HER2, HER3, HER4, as well as heterologous receptor systems such as integrin  $\beta$ 1, integrin  $\beta$ 3, EPHA2, and the urokinase-type plasminogen activator

receptor or directly with signaling molecules such as SRC is another way for the cancer cells to escape the effects of EGFR inhibition (23–26). Removal of EGFR by Sym004 will also eliminate these interactions.

In conclusion, Sym004 has a mechanism of action that is different from that of approved mAbs. Due to its distinctive mechanism of action, Sym004 has superior anticancer activity in EGFR-dependent tumor xenografts and has the potential to treat tumors with acquired resistance to other EGFR-targeted agents, including both mAbs and small-molecule tyrosine kinase inhibitors. These results thus provide a clear rationale for evaluating Sym004 in clinical trials with human EGFR-positive cancers.

## References

1. Wong AJ, Ruppert JM, Bigner SH, et al. Structural alterations of the epidermal growth factor receptor gene in human gliomas. *Proc Natl Acad Sci U S A* 1992;89:2965–9.
2. Damstrup L, Kuwada SK, Dempsey PJ, et al. Amphiregulin acts as an autocrine growth factor in two human polarizing colon cancer lines that exhibit domain selective EGF receptor mitogenesis. *Br J Cancer* 1999;80:1012–9.
3. Peghini PL, Iwamoto M, Raffeld M, et al. Overexpression of epidermal growth factor and hepatocyte growth factor receptors in a proportion of gastrinomas correlates with aggressive growth and lower curability. *Clin Cancer Res* 2002;8:2273–85.
4. Arteaga CL. The epidermal growth factor receptor: from mutant oncogene in nonhuman cancers to therapeutic target in human neoplasia. *J Clin Oncol* 2001;19:32–40S.
5. Mendelsohn J, Baselga J. Epidermal growth factor receptor targeting in cancer. *Semin Oncol* 2006;33:369–85.
6. Rivera F, Vega-Villegas ME, Lopez-Brea MF, Marquez R. Current situation of panitumumab, matuzumab, nimotuzumab and zalutumumab. *Acta Oncol* 2008;47:9–19.
7. Li S, Schmitz KR, Jeffrey PD, et al. Structural basis for inhibition of the epidermal growth factor receptor by cetuximab. *Cancer Cell* 2005;7:301–11.
8. Kurai J, Chikumi H, Hashimoto K, et al. Antibody-dependent cellular cytotoxicity mediated by cetuximab against lung cancer cell lines. *Clin Cancer Res* 2007;13:1552–61.
9. Prewett M, Rockwell P, Rockwell RF, et al. The biologic effects of C225, a chimeric monoclonal antibody to the EGFR, on human prostate carcinoma. *J Immunother Emphasis Tumor Immunol* 1996;19:419–27.
10. Friedman LM, Rinon A, Schechter B, et al. Synergistic down-regulation of receptor tyrosine kinases by combinations of mAbs: implications for cancer immunotherapy. *Proc Natl Acad Sci U S A* 2005;102:1915–20.
11. Ben-Kasus T, Schechter B, Lavi S, Yarden Y, Sela M. Persistent elimination of ErbB-2/HER2-overexpressing tumors using combinations of monoclonal antibodies: relevance of receptor endocytosis. *Proc Natl Acad Sci U S A* 2009;106:3294–9.
12. Meijer PJ, Andersen PS, Haahr HM, et al. Isolation of human antibody repertoires with preservation of the natural heavy and light chain pairing. *J Mol Biol* 2006;358:764–72.
13. Hirabayashi K, Yano J, Inoue T, et al. Inhibition of cancer cell growth by polyinosinic-polycytidylic acid/cationic liposome complex: a new biological activity. *Cancer Res* 1999;59:4325–33.
14. Brattain MG, Levine AE, Chakrabarty S, et al. Heterogeneity of human colon carcinoma. *Cancer Metastasis Rev* 1984;3:177–91.
15. Li L, Heldin CH, Heldin P. Inhibition of platelet-derived growth factor-BB-induced receptor activation and fibroblast migration by hyaluronan activation of CD44. *J Biol Chem* 2006;281:26512–9.
16. Pedersen MW, Pedersen N, Ottesen LH, Poulsen HS. Differential response to gefitinib of cells expressing normal EGFR and the mutant EGFRvIII. *Br J Cancer* 2005;93:915–23.
17. Tallarida RJ. An overview of drug combination analysis with isobolograms. *J Pharmacol Exp Ther* 2006;319:1–7.
18. Sorkin A, Kornilova E, Teslenko L, Sorokin A, Nikolsky N. Recycling of epidermal growth factor-receptor complexes in A431 cells. *Biochim Biophys Acta* 1989;1011:88–96.
19. Sorkin A, Krolenko S, Kudrjavtceva N, et al. Recycling of epidermal growth factor-receptor complexes in A431 cells: identification of dual pathways. *J Cell Biol* 1991;112:55–63.
20. Huang F, Kirkpatrick D, Jiang X, Gygi S, Sorkin A. Differential regulation of EGF receptor internalization and degradation by multiubiquitination within the kinase domain. *Mol Cell* 2006;21:737–48.
21. Barbieri MA, Roberts RL, Gumusboga A, et al. Epidermal growth factor and membrane trafficking. EGF receptor activation of endocytosis requires Rab5a. *J Cell Biol* 2000;151:539–50.
22. Deb TB, Su L, Wong L, et al. Epidermal growth factor (EGF) receptor kinase-independent signaling by EGF. *J Biol Chem* 2001;276:15554–60.
23. Larsen AB, Pedersen MW, Stockhausen MT, et al. Activation of the EGFR gene target EphA2 inhibits epidermal growth factor-induced cancer cell motility. *Mol Cancer Res* 2007;5:283–93.
24. Moro L, Dolce L, Cabodi S, et al. Integrin-induced epidermal growth factor (EGF) receptor activation requires c-Src and p130Cas and leads to phosphorylation of specific EGF receptor tyrosines. *J Biol Chem* 2002;277:9405–14.
25. Liu D, Aguirre GJ, Estrada Y, Ossowski L. EGFR is a transducer of the urokinase receptor initiated signal that is required for *in vivo* growth of a human carcinoma. *Cancer Cell* 2002;1:445–57.
26. Lu Y, Li X, Liang K, et al. Epidermal growth factor receptor (EGFR) ubiquitination as a mechanism of acquired resistance escaping treatment by the anti-EGFR monoclonal antibody cetuximab. *Cancer Res* 2007;67:8240–7.

## Disclosure of Potential Conflicts of Interest

No potential conflicts of interest were disclosed.

## Acknowledgments

The costs of publication of this article were defrayed in part by the payment of page charges. This article must therefore be hereby marked *advertisement* in accordance with 18 U.S.C. Section 1734 solely to indicate this fact.

Received 4/21/09; revised 10/14/09; accepted 11/6/09; published OnlineFirst 1/12/10.